

THE DISCOVERY OF HYDROTHERMAL VENTS

25th Anniversary CD-ROM

The Galápagos Rift at 86° W: Volcanism, Structure, and Evolution of the Rift Valley

by

Tjeerd H. van Andel and Robert D. Ballard

Reprinted from the *Journal of Geophysical Research*,
Vol. 84, No. 810: 5390-5406
September 10, 1979

Reprinted with permission from authors and AGU Publications
© 1979 American Geophysical Union



Printed from "The Discovery of Hydrothermal Vents - 25th Anniversary CD-ROM"
©2002 Woods Hole Oceanographic Institution

THE GALAPAGOS RIFT AT 86°W:
2. VOLCANISM, STRUCTURE, AND EVOLUTION OF THE RIFT VALLEY

Tjeerd H. van Andel

Department of Geology, Stanford University, Stanford, California 94305

Robert D. Ballard

Woods Hole Oceanographic Institution, Woods Hole, Massachusetts 02543

Abstract. This paper presents part of the data obtained during a multidisciplinary study of the Galapagos Rift in the western Panama Basin. It is based on photographic traverses made by the Angus towed camera system, observations made from the DSRV Alvin, and bathymetric maps constructed by the U.S. Navy using a multi-narrow-beam sonar system. The area studied is a 9-km section of the rift valley at 86°W on the crest of a long and uncomplicated segment of the Galapagos Rift. In contrast to the terraced rift valley of the Mid-Atlantic Ridge, the Galapagos rift valley consists of a single trough, a few hundred meters deep, between faulted walls leading to low crestral ranges. The center of the rift valley contains a broad depression of sheet flows at the geometric axis and a lobate ridge of low volcanoes of pillow flows to the north. The volcanic ridge is highly fissured and contains several hydrothermal springs on pillowed terrain adjacent to depressions containing young sheet flows. The youngest sheet flows may be less than 100 years old, while the entire age range of the young volcanic complex can be estimated at no more than a few thousand years. The young volcanic complex is bordered to the north and south by block-faulted marginal ridges that are significantly older. A model is proposed for the volcanic and structural evolution of the rift valley that begins with a zone of rapid extension, subsidence along boundary faults, and copious flows of sheet lavas from a shallow magma chamber (0.5-1.0 km). After the crust has thickened, subsidence, extension, and flow rates decrease, and a ridge of small pillowed volcanoes is formed. A new axis of extension then develops to one side or the other of the volcanic ridge. This area begins to subside and fill with sheet flows. The older volcanic ridge is accreted to the nearest marginal high and straightened by normal faults. This complex then undergoes uplift and evidently becomes the crestral range, as the previous crestral range is rafted outward and gradually subsides.

The Galapagos Rift Hydrothermal Project

The Galapagos Rift extends eastward from a triple junction with the East Pacific Rise (Figure 1). It passes north of the Galapagos Islands, enters the western Panama Basin between the Cocos and Carnegie ridges, and terminates against the Panama fracture zone at 83°W (van Andel et al., 1971). The rather complex history

of this region has most recently been discussed by Hey (1977) and Hey et al. (1977).

The Galapagos Rift forms the boundary between the Cocos and Nazca plates. Between 90° and 85°W the rift is uninterrupted by major fracture zones, but farther east it is offset northward about 350 km across several closely spaced transform faults. The first detailed study of the rift crest in the western Panama Basin was carried out in 1972 with surface ship and deep towed geophysical methods (Sclater and Klitgord, 1973; Klitgord and Mudie, 1974; Sclater et al., 1974; Detrick et al., 1974; Williams et al., 1974). This study centered on the crest at 86°W and indicated probable convective cooling of the crust by circulating seawater, raising the possibility that submarine hydrothermal springs might occur in the area. For that reason a multidisciplinary project, funded by the International Decade of Ocean Exploration of the National Science Foundation, was developed to locate such springs, study the nature of their hydrothermal waters and associated precipitates, and investigate the processes of seawater circulation in newly formed oceanic crust. In the summer of 1976, as a part of this study, surface ship investigations were carried out in the rift valley at 86°W and the adjacent southern flank using deep-towed geophysical instrumentation, heat flow probes, sediment corers, and bottom water samplers. The results of this investigation have been reported by Crane (1978), Weiss et al. (1977), and Lonsdale (1974, 1977).

Subsequently, a major expedition in the winter of 1977 examined the rift valley and south flank using the submersible Alvin and the Angus deep-towed camera system as well as other surface ship techniques (Corliss et al., 1979). In this paper we discuss the results of geological studies of the rift valley designed to provide the background for the geochemical investigations of the hydrothermal springs that were found in the valley. In other papers in this series the nature and origin of extensive sheet flows in the rift valley (Ballard et al., 1979), the regional structure and morphology of the Galapagos Rift (Allmendinger and Riis, 1979; Crane, 1979), and the detailed geology of the hydrothermal springs in the rift valley (Crane and Ballard, 1979) are also examined.

The Geological Data

For this study we have available four separate sets of data: detailed bathymetric charts constructed by the U.S. Navy Oceanographic Office using a General Instrument multinarrow beam sonar system (SASS), a photographic survey conducted

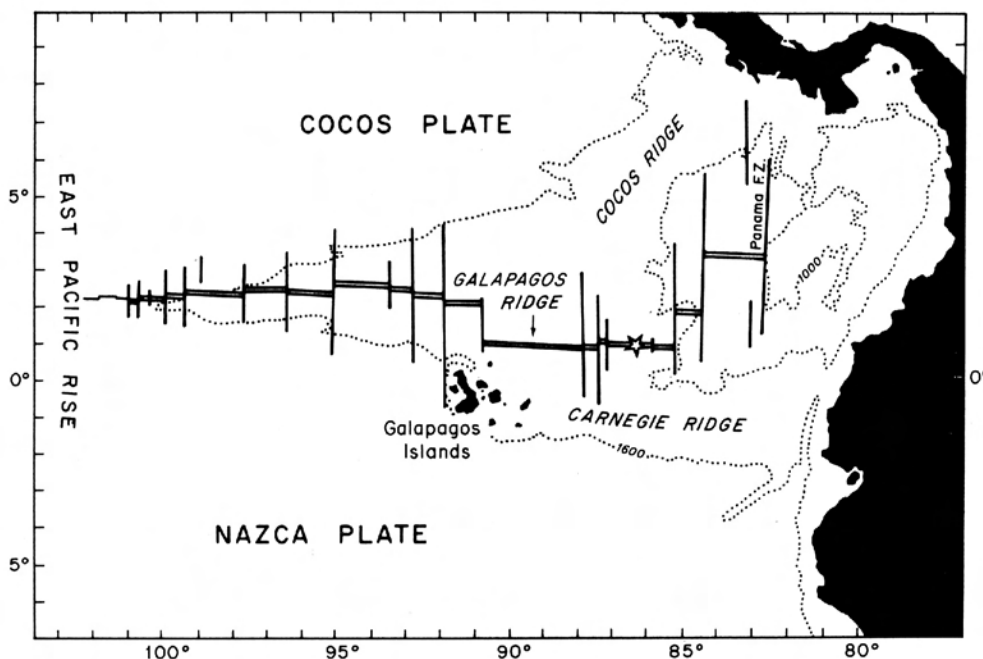


Fig. 1. Location of Galapagos Rift study area (star) in the western Panama Basin. Modified after Hey (1977, Figure 1). Contours are in fathoms (1 fathom = 1.83 m).

by the deep-towed Angus camera system of the Woods Hole Oceanographic Institution, direct visual observations and photographs taken from the submersible Alvin, and the results of the 1972 and 1976 Scripps Institute of Oceanography Deep-Tow survey. The later data set consists of detailed bathymetric profiles, side scan sonar records, and bottom photographs (Crane, 1978; Lonsdale, 1977). We have especially made use of the structural information made available by Crane (1978).

Bathymetric survey. On behalf of the project a detailed bathymetric survey was carried out in the spring of 1976 with a multi-narrow-beam sonar (SASS) over the region between 85°12' and 86°17'W and 0°25' and 0°01'N. This survey system, described by Glenn (1970) and Phillips and Fleming (1978), provides essentially complete insonification of the sea floor along 304-km-wide parallel overlapping strips and permits the construction of very detailed and highly precise bathymetric maps. The regional versions of these charts have been discussed by Allmendinger and Riis (1979) and Crane (1979). For the rift valley segment discussed in this paper we have prepared a chart on a scale of 1:8000 with a 2-fathom (3.66 m) contour interval for the area between 86°06' and 86°11'W and 0°46' and 0°49'N.

Angus deep-towed photographic survey. The Angus camera system consists of a large capacity Benthos survey camera capable of taking 2900 35-mm color pictures per lowering. The repetition rate during the program varied from 8 to 16 sec per frame, and the tow speed ranged between 0.5 and 1 knot. The picture radius is 6 m when flown at a preferred altitude of 4 m. In all, about 150 km of sea floor were photographed, yielding about 57,000 bottom pictures. After each lowering was completed, the film was immediately processed in a film laboratory aboard the ship. Since the film used produced a positive print when developed, the reel could be viewed

immediately after processing. In the lower corner of each frame is a light-emitting diode display of the precision time base used by the tracking system, making it possible to locate each picture precisely in a three-dimensional frame of reference. The camera was navigated using the same acoustic transponder system that tracked Alvin. It was therefore possible to vector the submersible to various bottom targets located by Angus. Pressure-depth sensor and acoustic altitude data were combined with the navigational information to produce detailed microtopographic profiles of the terrain that was photographed. For the rift valley we have used 12 long Angus runs; six others provide detailed coverage of hydrothermal spring sites, as discussed by Crane and Ballard (1979).

Alvin dive data. With the exception of the geochemical sensing and sampling system that need not concern us here, the Alvin instrument configuration and operational procedures were the same as those described by Ballard and van Andel (1977a) for the French-American Mid-Ocean Undersea Study (Famous) project. The Alvin data relevant to our study consist of written logs of the scientific observers and photographs taken with the external 35-mm color camera system. The latter are a useful complement to the Angus photographs because the Alvin cameras view the terrain at an angle of 60° from the vertical instead of straight down.

The Alvin depth and altitude data were recorded within the pressure sphere on a Geosecs recorder. Unfortunately, no listing of these data is available yet. Hence a final edit of the Alvin tracks and the very important Alvin microtopographic profiles are not available at this time. This is particularly regrettable because several Alvin tracks are perpendicular to the strike of the ridge axis in contrast to the subparallel Angus runs. Of the 18 Alvin dives in the rift valley we have used eight that

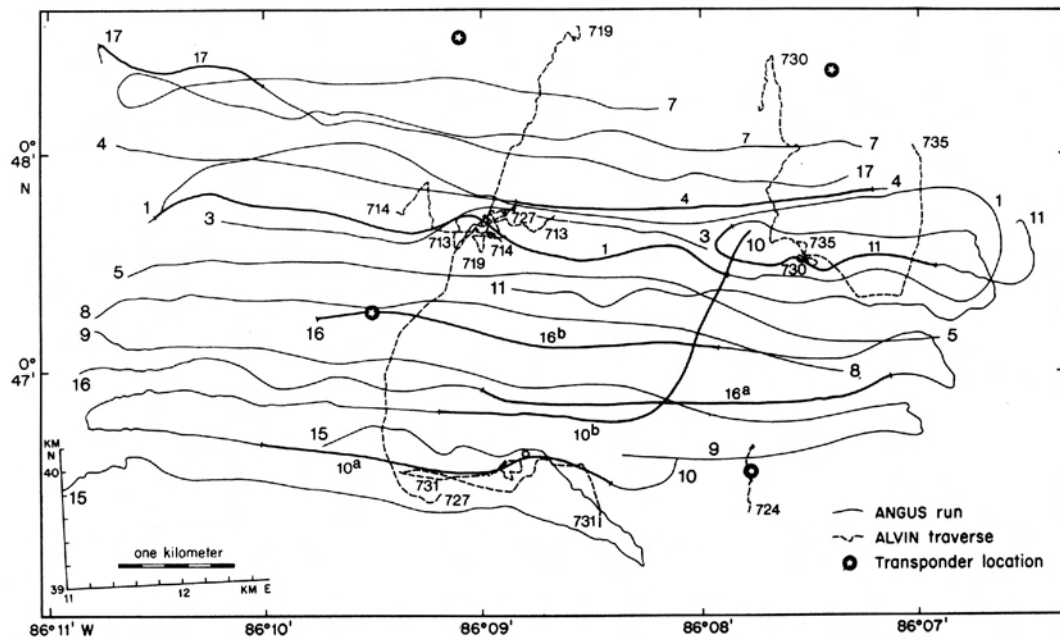


Fig. 2. Track chart of Angus and Alvin traverses used in this study. Locations of transponder net are shown, with adjusted coordinate net in the lower left corner. Tracks represent second-order adjustment to the topography of Figure 3 (see text). Heavy, numbered lines are profiles of Figure 6. Latitude and longitude from multi-beam survey.

cover appreciable distances; the others are restricted to the immediate vicinity of the hydrothermal springs. The Alvin color photographs were reviewed and described in the same manner as the Angus photographs.

Navigation. Two different navigation systems and three separate frames of reference control the data sets used in this study. The multibeam bathymetric survey was controlled by satellite and inertial navigation. Within each survey strip, about 2 km wide at the mean area depth, all data points are rigidly fixed and subject only to distortion along the track (probably no more than a few tens of meters) resulting from errors in the estimate of the ship's speed. Larger distortions may occur at the edges of adjoining strips, since the outer beams are traveling a greater distance through the water, resulting in greater acoustical errors. Such errors are minimized, since the strips overlap and the outer beams, in many instances, need not be used in constructing the map. Five strips cover the study area, centered at approximately 86°06', 86°08', 86°10', and 86°10.5'W.

The Angus and Alvin tracks were navigated with pairs of anchored acoustic transponders chosen from a set of four (Figure 2), with positions recorded in an arbitrary coordinate system in meters east and north from an origin well outside the area. Given perfect knowledge of the relative positions of all transponders, successive points along a track can be determined to within 10–20 m under favorable circumstances (Ballard and van Andel, 1977a). However, small errors in the length and azimuth of the base lines between transponder pairs give rise to distortions that depend on the pair chosen and the location of the point with respect to the base line. Because Alvin often hugs the bottom, its navigation tends to be less accurate than

that of the Angus sled, which has its relay transponder located 300 m above bottom. The Scripps Deep-Tow survey of 1976 was also navigated with a transponder net connected, somewhat tenuously, with the 1977 net by means of a single transponder left in the area. Adjustments based on topography were needed to bring the two nets in concordance.

As in the Famous project (Ballard and van Andel, 1977a), we have adjusted the Angus/Alvin Deep-Tow tracks to the bathymetric chart because the latter has the greater internal consistency and is, with so much data, more difficult to adjust. In order to do so we constructed a bathymetric chart from the Angus microtopographic profiles after first reconciling crossover discrepancies in topography and geology. This chart was then fitted to the multibeam bathymetric chart by translation and rotation, yielding the relation between the coordinate system and the latitude and longitude shown on Figure 2. We then removed remaining minor topographic discrepancies by adjusting parts of runs, primarily runs 3, 4, 10, and 17. Alvin tracks were further adjusted with approximate depth profiles computed from the navigation data and the locations of hydrothermal springs. Their positions on Figure 2 are not final. Finally, third-order adjustments, not shown on Figure 2, were made by adjusting geological observations and fine-scale microtopography. Because of their subjective nature, these adjustments only affect Plate 2.

Setting, Morphology, and Structure of the Rift Valley

The morphology of the Galapagos Rift at 86°W is simple, consisting of a rift valley with a mean depth of 2500 m and a width of about 3.5 km

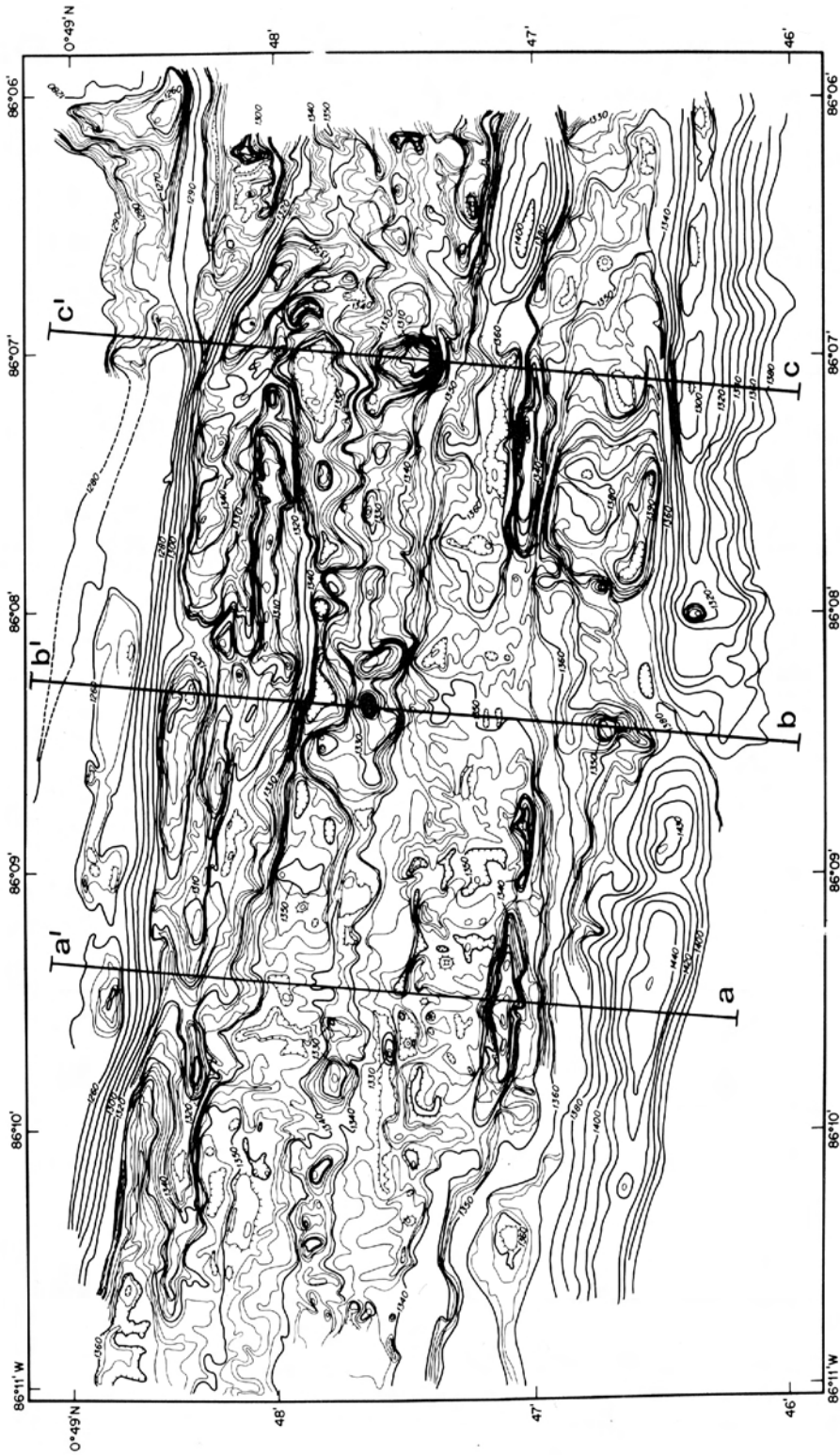


Fig. 3. Bathymetric chart of the rift valley at 86°W based on multi-narrow-beam survey by U.S. Navy Oceanographic Office. Contours in fathoms, contour interval generally 2 fathoms (3.66 m). Labeled lines are profiles of lower half of Figure 4.

in the center of the study area (Figure 3). The valley is bordered by steep slopes which lead directly to crestral ranges (the first line of hills beyond the valley), elevated from 100 to 250 m above the valley floor (Figure 4). Outward, the crestral ranges drop steeply into boundary troughs beyond which the ridges gently slope outward, closely following the subsidence curve of Sclater and Francheteau (1970). The morphology at 86°W is characteristic of the entire rift valley segment for which we have detailed data. This segment extends from 86°17'W to 85°25'W, where the axis terminates against a major transform fault. Over this distance the rift valley narrows, and the difference in elevation between valley floor and crestral ranges decreases eastward (Allmendinger and Riis, 1979).

The simplicity of the Galapagos Rift crest contrasts with the complex crest and rift valley of the Mid-Atlantic Ridge (Needham and Franche-

teau, 1974). There, the walls of the inner rift valley lead to two successively higher terraces on either side before an outer wall rises to the crestral ranges. The distance between outer walls ranges from 25 to 30 km (Macdonald et al., 1975; Ramberg and van Andel, 1977), and the difference in elevation between the inner valley floor and range crest is 1500–2500 m. The inner valley floor, the morphological analog of the Galapagos Rift valley, has about the same width but a much higher relief, with walls ranging from 300 to 700 m in height. This complex Mid-Atlantic Ridge rift system represents the same volcanic and structural evolution accomplished on the Galapagos Rift in the 5-km width and 250-m elevation of the crestral ranges and rift valley.

In detail, the Galapagos Rift valley is similar to the inner rift valley of the Mid-Atlantic Ridge in the Famous area (Macdonald et al., 1975; Ballard and van Andel, 1977b), consisting of a north wall, northern marginal high, marginal

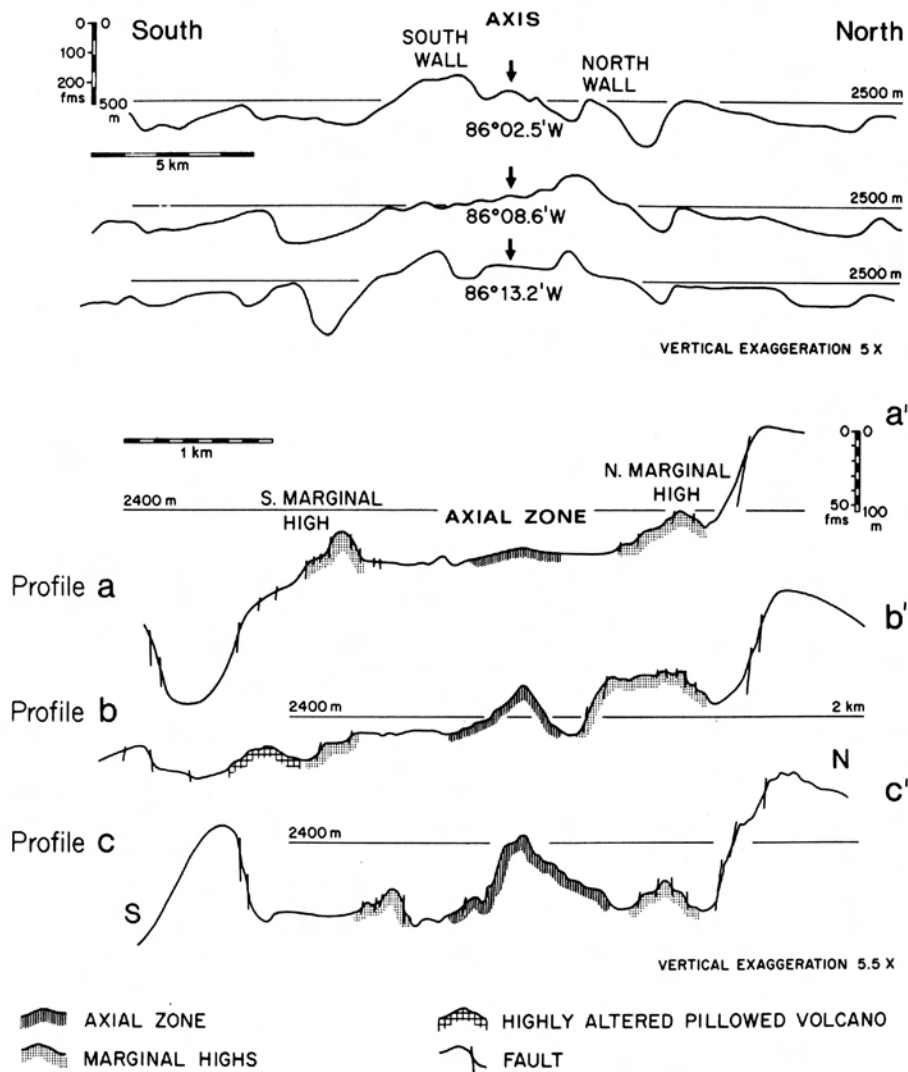


Fig. 4. Topographic profiles perpendicular to rift axis in crestral area at 86°W. (Top) Three profiles extending out to ridge flanks constructed from bathymetric chart at a scale of 1:36,000 with 5-fathom (9.15 m) contour interval; azimuth N15°E, position at axis crossing shown. (Bottom) Profiles of rift valley constructed from bathymetric chart having scale of 1:8000 with 2-fathom contour interval; positions on Figure 3.

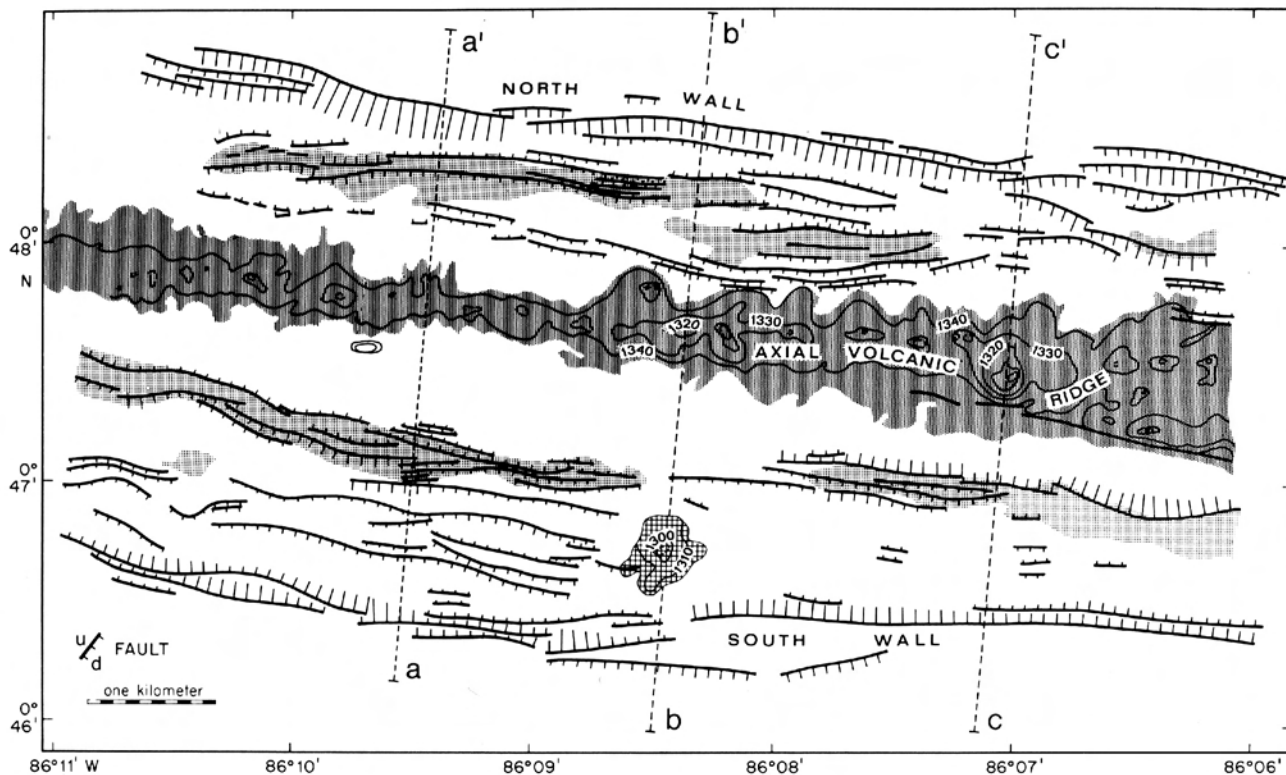


Fig. 5. Physiographic and structural map of the rift valley at 86°W. Fault patterns from Alvin observations, bathymetry, and deep-tow data after Crane (1978). Present volcanic axis and marginal highs indicated with shading. Contours on axial high and seamount in south central region are in fathoms (1.83 m). North and south wall faults have been simplified. Legend same as in Figure 4. Length of hachures on fault lines schematically indicates height of fault scarp.

trough, central volcanic high, southern marginal trough and high, and south wall (Figures 3, 4, and 5). The axial high, about 0.5-1.0 km wide and rising from 20 to 60 m above the adjacent floor, is characterized by lobate contours resulting from constructional volcanism. The terrain is fissured but not faulted. Beyond the featureless marginal depressions, the contours are markedly straightened by faulting and uplift (Figure 3). On the north side the block-faulted marginal high is crowded closely between the axial ridge and north wall. On the south side the marginal high is separated from the axial ridge by a 0.5- to 0.8-km-wide depression and from the south wall by a deep trough. In the east this trough is wide and shallow. In the west it is a steep-walled graben with a maximum depth of about 200 m. A small seamount occurs between the eastern and western parts of the trough opposite an offset of the south wall of about 0.5 km.

The fault pattern is subparallel to the axis, but individual faults deviate as much as 30° from the strike of the rift and are distinctly en echelon, giving rise to an echelon horsts and grabens in the marginal highs (Figure 5). Throws range from 10 to 60 m and occasionally are 100 m (Crane, 1978).

Over the last 3 m.y. the opening rate of the Galapagos Rift has averaged 70 mm/yr and has been nearly symmetrical (south side 0.5 mm/yr faster) with respect to the center of the Brunhes anomaly which lies close to the north wall (Klitgord and

Mudie, 1974, Figure 14). With this opening rate the crustal age at the walls should be about 100,000 years, and the entire structural evolution, represented by the outer side of the walls, would be completed in less than 150,000 years. Even with a zone of acceleration equal in width to the axial volcanic zone, this evolutionary period would only be lengthened by about 15%. In contrast, the walls of the inner rift in the Famous area are on crust of 150,000 years, and the tectonic evolution is complete at the edge of the crestal ranges in about 2 m.y.

The spreading symmetry of the Galapagos Rift does not correspond to a morphological or structural symmetry (Figures 4 and 5). The volcanic axis lies well north of the geometric axis, and the southern marginal zone is much wider and lower than the northern one. On a broader scale a marginal high on one side of the axis commonly corresponds to a depression at the foot of the opposite slope (Crane, 1978), and highs and lows alternate along strike in the marginal zones of the valley and along the crestal ranges. Even the axial zone shows along-strike variation in width, elevation (Figures 4 and 5), and even age (see below). This pattern of highs and lows alternating along strike in the axial valley extends over the entire surveyed area from 85°25'W to 86°17'W (Allmendinger and Riis, 1979).

On the largest scale the flanks of the Galapagos Ridge consist of alternating bands of high and low terrain which are highly linear

and strike parallel to the rift axis, called lineaments by Allmendinger and Riis (1979). Internally, each lineament consists of an echelon blocks separated by faults which trend at low angles to the strike of the lineament. These faults are analogous to the faults that border the components of the marginal highs within the rift valley. The topographic similarity of lineaments at corresponding distances north and south of the ridge axis is excellent, including even minor details such as abundance of small seamounts. In addition, a high in a lineament on one side of the crest always corresponds to a depression in the opposing lineament on the other side, recalling the across-axis alternation of highs and lows in the rift valley. The flank lineaments, which have the same width as the marginal zones of the rift, thus resemble their basic morphology, although on a much reduced vertical scale. Counting toward the axis, all lineaments are paired on opposite sides, except for the youngest one on the south side, which must be taken as corresponding to a new lineament now forming between the volcanic axis and the north wall. Consequently, Allmendinger and Riis (1979) have postulated that lineaments are formed, alternately in the northern and southern marginal zone, as the axial volcanic ridge migrates to one side or the other and begins its structural evolution as a marginal high and depression complex. Its structural evolution is completed when the lineament reaches the crestal range. Subsequently, the lineament travels passively outward, being modified only by subsidence and relief reduction along normal faults.

Construction of the Geological Map

The photographic and observational data permit the construction of a detailed geological map of the rift valley floor. Given the track spacing (Figure 2) and the photoarea of about 12-20 m² each, the coverage is not complete, and interpolation is necessary. This interpolation is possible because of known relations between lava types and microtopography.

Map categories. Two basic flow forms are present within the rift valley: pillow flows and sheet flows. The various types of pillow flows are similar to those previously described by Ballard and Moore (1977) for the rift valley of the Mid-Atlantic Ridge. The most common pillow forms include bulbous and flattened pillows, while elongated pillows are less common than in the Famous area. The various types of sheet flows are far less known and have only recently been described in any detail (Ballard et al., 1979). Since sheet flows are less understood, a brief description of their flow forms is given. Photos of lava types are given by Ballard et al. (1979).

One of the most common forms is a flat lobate sheet flow which has a gentle hummocky relief. This form resembles a flattened pillow but lacks its characteristic striations and bread crust surface texture. The flat flow is a smooth pavement surface, its microrelief being no greater than a few centimeters. Other sheet flow forms appear to have been initially flat and later deformed and folded to varying degrees.

Some have long linear folds (folded flow), while others exhibit greater deformation (rippled flow), and still others contain circular patterns (whorly flow). Two extreme forms exist which are similar in appearance to subaerial aa flows but whose origins are quite different. These include hackly flows and jumbled flows. Hackly flows are irregular, blocky units consisting of brittle glassy masses. Jumbled flows, although similar looking, are not as chaotic as the hackly flows and commonly have closely spaced folds.

In addition to these flow types the presence of rubble, talus, fissures (with depth, width, and orientation when possible), scarps, faults, flow fronts, flow directions, and collapse features were recorded.

An important element in reconstructing the history of the rift valley floor is the age of the various flow units. Because the entire floor is younger than 100,000 years, K-argon dates are not useful. Other dating techniques such as fission tracks (Storzer and Selo, 1974) and rates of accumulation of manganese crust and palagonitization (Hekinian and Hoffert, 1975; Bryan and Moore, 1977) are not yet available from the few samples collected in the area and, in the past, have yielded contradictory results (Ballard and van Andel, 1977b). Consequently, we have developed a scheme of dating based upon the relative ages of flow units determined by the abundance and freshness of volcanic glass, the degree of alteration of the volcanics, and the sediment cover. These, of course, are subjective criteria that are not easily quantified and are affected by factors other than age alone. Freshness and abundance of glass and the degree of alteration are also a function of magma composition and eruption processes. Sediment cover, even with a uniform particle rain from the ocean surface, varies with topography as a result of ubiquitous downslope transport. Thus even old but steep slopes may be sediment free, while anomalously thick accumulations may occur at the foot of the scarps and in hollows and depressions. The microtopography of the flows affects the amount of sediment cover: flat sheet flow surfaces are completely covered with a few centimeters of sediment, while large pillows are partially exposed through a sediment blanket a meter thick. Before assigning ages, we have attempted to correct for such factors.

Fortunately, relative age assignments can often be confirmed at contacts where sediment cover or the degree of alteration abruptly changes, or where one flow overlaps an older flow. By tracing and cross-correlating contacts between tracks we have achieved a scheme of relative age assignments in which we have reasonable confidence. However, assignment of a flow unit to a certain age category in different parts of the map implies only the same relation to surrounding units, not precise age equivalence. The original records use a fivefold age subdivision, but corrections for external factors and the need to define mappable units have reduced this to three age units for the pillow flows, two for the sheet flows in the volcanic axial region, and a single age unit for the older, faulted, marginal areas where the sediment cover ranges from 50 to 100%.

The youngest category consists of fresh, very

glassy pillows and sheet flows which commonly show strong specular light reflections and are sediment free or have a light dusting of scattered particles. Older units show loss of glass by spalling, initial alteration of the lava surfaces, and moderate dusting with sediment contained in small ponds between pillows or folds in the sheet flows. Although sheet flows of this category occur in various places, especially south of the axial ridge, we have not been able to locate clear contacts between units of youngest and intermediate age, and hence we use only a single sheet flow age category equivalent to the two youngest pillow categories. Most of the sheet flows are probably equivalent in age to the youngest pillow flows.

The oldest lava flows in the center of the valley have lost most of their glass, commonly show alteration and manganese encrustation, and have a sediment cover ranging from heavily dusted to 25-50% of the surface area.

The boundary between the young rocks of the axial region and those of the valley margins is distinct and marked by an abrupt increase in

sediment cover to 75-100% of the surface area. The sediment is also much thicker. The micro-relief of the sheet flows tends to be completely buried, and over large areas, only the tops of pillows protrude. In this area the distinction between the two basic flow types can only be made by looking in open fissures which cut through both the rock and its sediment cover.

The large change in sediment cover suggests a major age break between the axial and marginal areas. The boundary generally coincides with initial faulting and uplift of the marginal highs. However, a thick sediment cover occasionally occurs without clear topographic limits (Figure 6, profile 16a), possibly as a result of re-sedimentation below an adjacent high. In such cases an assignment to the oldest age category remains in doubt.

An estimate of the real ages is difficult to obtain. The sedimentation rate in the Panama Basin is high owing to a very high surface productivity, the winnowing of sediment on surrounding plateaus, and subsequent downslope transport (Moore et al., 1973; van Andel, 1973).

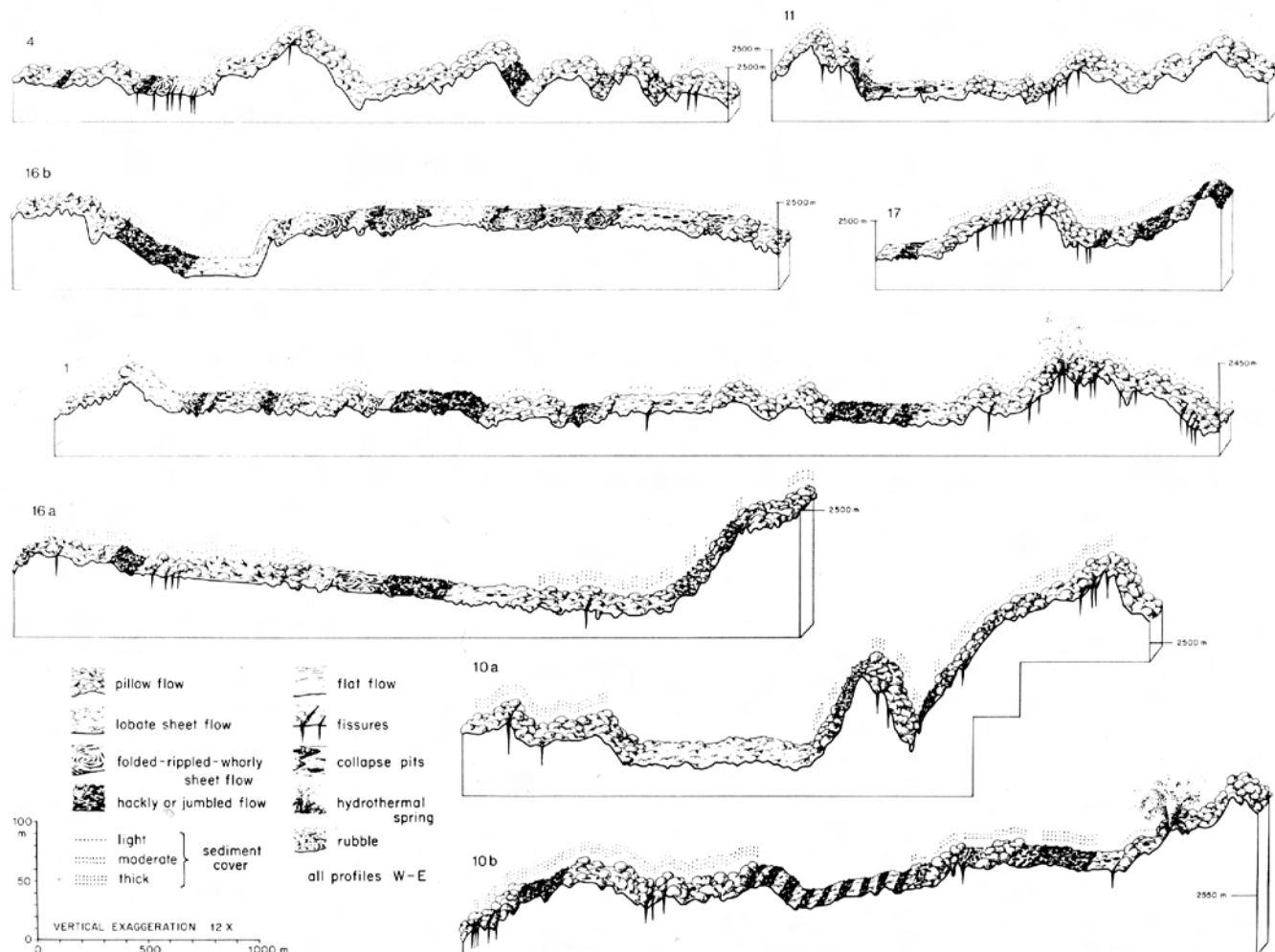


Fig. 6. Microtopography and geology along selected Angus runs representative of prime data used for Figure 7. Position of traverses shown on Figure 2. Rock units have been plotted as observed without simplification except for reasons of space. Sediment cover shown simplified in three categories instead of the original five. Relative age categories are not shown. Reference depth in meters given for each profile.

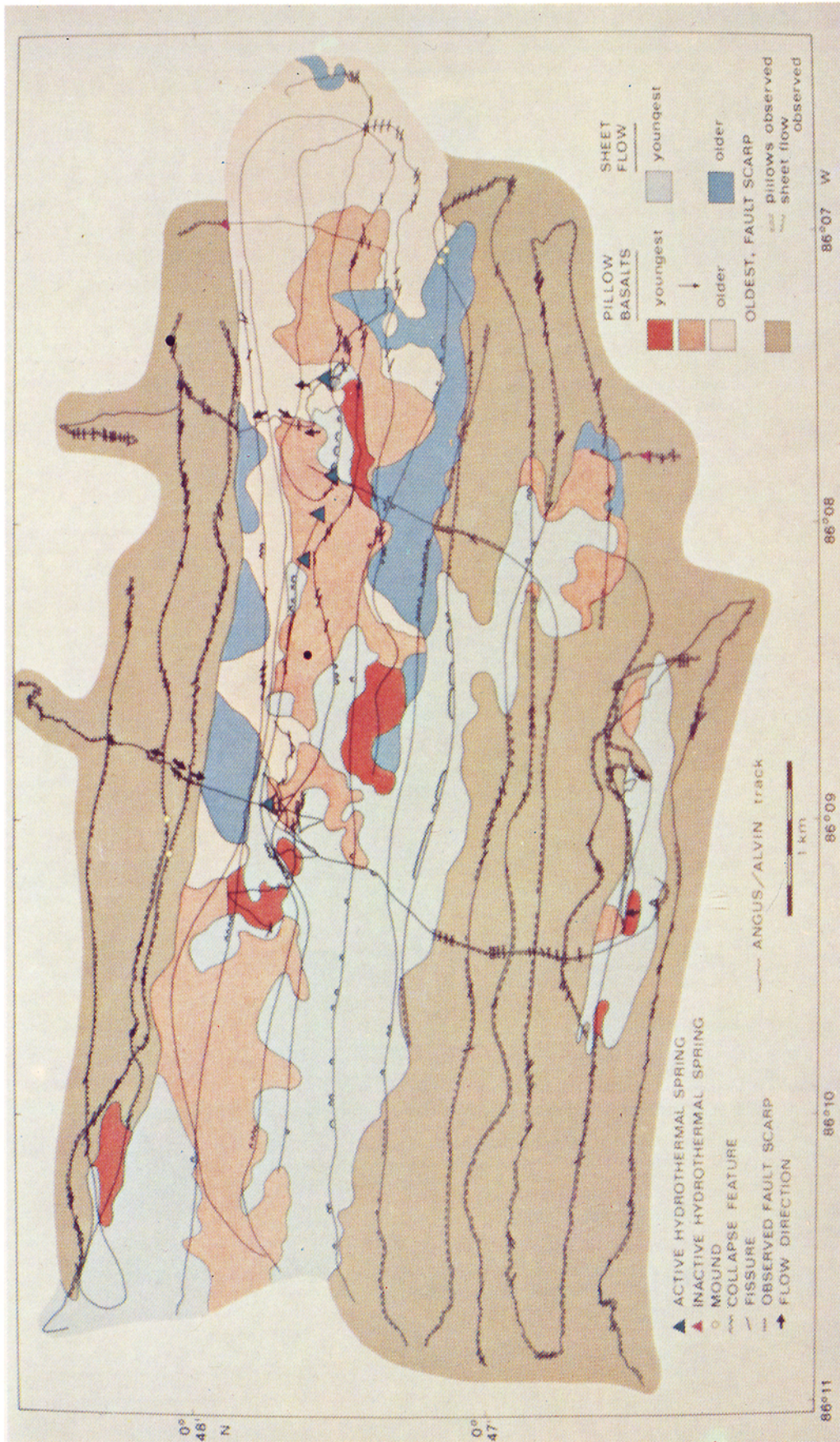


Plate 1. Geologic map of the rift valley. Based on profiles such as Figure 6, but categories have been simplified for the sake of mappability, and relative age assignments added as described in the text. See text for explanation.

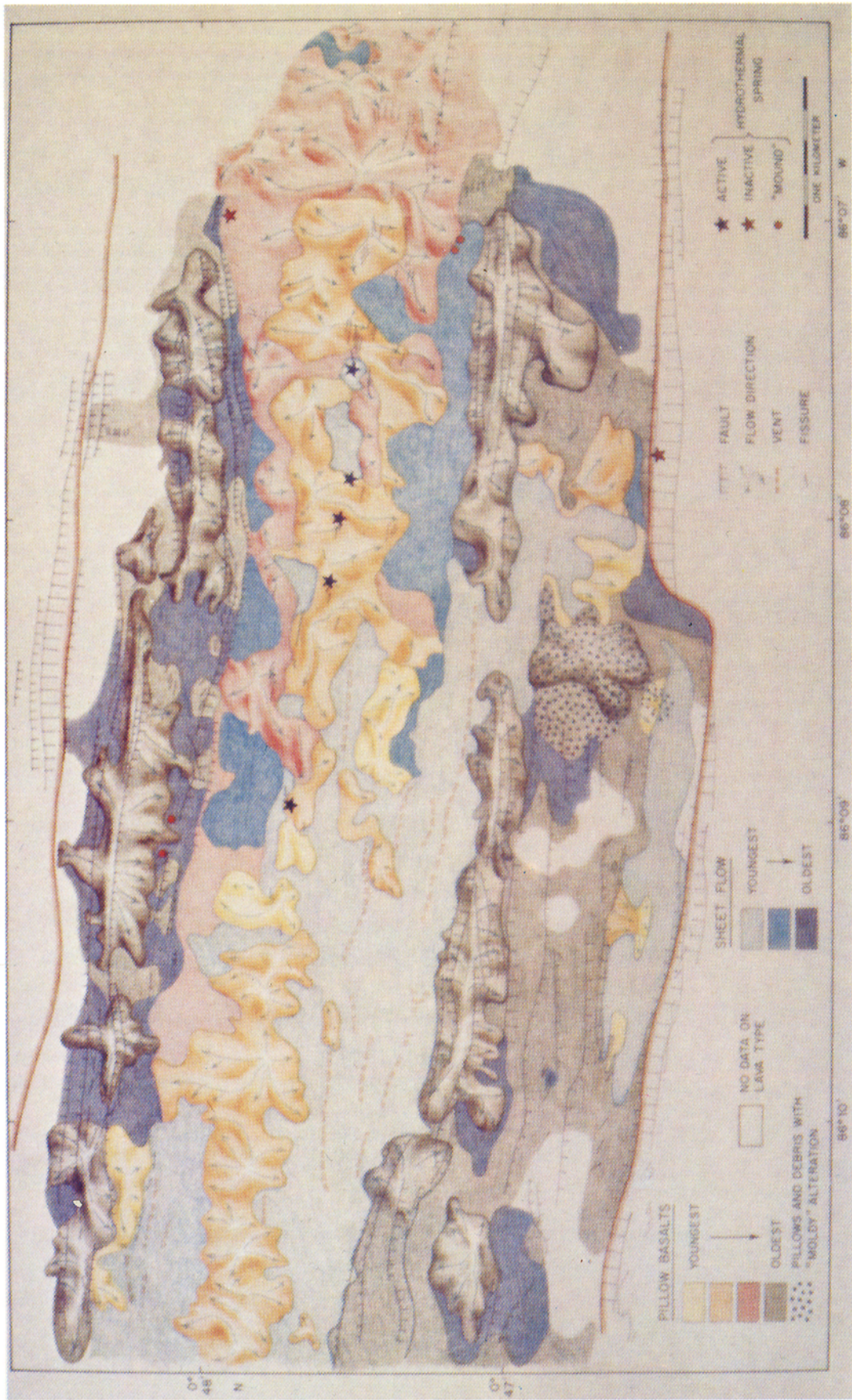


Plate 2. Interpretative diagram of the geology of the inner rift valley. Basic rock types and ages from Plate 1. Volcano forms and flow directions from analysis of the bathymetry, supported by observations of flow directions by Alvin. Map includes third-order adjustment of data to bathymetry. Faults from Figure 5 and Alvin observations. Pattern of sheet flows and pillow basalts in marginal terrain extrapolated by means of topography from track data shown on Plate 1.

The mean long-range sedimentation rate over several million years in the eastern equatorial Pacific is about 1-2 cm/1000 yr (van Andel et al., 1975). This, however, is a minimum for the study area because of the shallow depth, greater productivity, and significant redeposition in the Panama Basin. Sediment thickness and crustal age on the south flank, some 30 km south of the axis of the Galapagos Rift at 86°W, indicate an average rate of 5 cm/1000 yr for the last several million years (Lonsdale, 1977). Variations in sedimentation, erosion, and dissolution rates during the Quaternary make this also a minimum value. Swift (1977), using radiocarbon dates and carbonate curves, has obtained much higher values for the Holocene in the western Panama Basin, with an average of 8 cm/1000 yr based upon eight cores obtained in the vicinity of the study area. Assuming that the true value is about 5 cm/1000 yr, the youngest (sediment free to lightly dusted) flow units must be much younger than 1000 years. Very glassy, highly reflective sheet flows, where dusting is virtually absent, are likely to be younger than a century. We therefore believe that the three youngest categories span a range from a few decades to a few thousand years.

Construction of the map. The data obtained from bottom photos were plotted on microtopographic profiles and tracks with a horizontal scale of 1:8000 and a vertical exaggeration of 12 times. Minor adjustments were then made at track crossings. After making a second-order fit of the tracks to the bathymetric chart the geologic map was constructed by interpolation using relations between rock types and microtopography that are evident from profiles like Figure 6. If overlain on the bathymetric chart, this geologic map (Plate 1) still shows third-order topographic discrepancies. Because further adjustment would be highly subjective, we have not corrected Plate 1 and have instead sketched a more interpretive geologic diagram which includes these adjustments (Plate 2) directly on the topographic base.

Geology of the Rift Valley

Three geologic zones coincide precisely with the structural zones in the rift valley and show a pronounced asymmetry. The northern marginal zone of older, sediment-covered flows is narrow, high, and crowded between the north wall and axial ridge. The southern marginal zone, however, is broad and lower and contains, in the deep troughs along the south wall, extensive and very young sheet flows. The axial zone consists of (1) a ridge of hilly terrain with lobate outlines mainly formed by pillow flows, (2) a broad depression to the south filled with young sheet flows spilling over into the troughs of the faulted southern marginal zone, and (3) a narrow northern zone of depressions with sheet flows alternating with spurs of pillow flows.

The axial ridge itself varies along its length in width, height, ruggedness, and age. It is broadest in the east, where it is composed of a cluster of pillowed volcanoes, up to 1 km long, several hundred meters wide, and rising as much as 60 m above the valley floor. The easternmost volcanoes are the oldest. Younger ones of simi-

lar dimensions occur along the south side of the axial ridge between 86°07' and 86°08'W. Westward, the older volcanoes are not present (or not exposed), and a gradually narrowing strip of young pillow volcanoes of indistinct shape and heights of 20-30 m forms the ridge between 86°08' and 86°09'W. Some of the youngest pillow flows observed form a flat shelf on the south flank between 86°08.5' and 86°09.5'W. The westernmost part of the axial ridge is low and rather featureless, consisting of young pillow flows which extend north to form a spur near 86°09.5'W. Similar alternation between highs and lows along strike in the axial ridge can be observed over the entire area of the multibeam survey.

The southern half of the axial region consists of an extensive low plain of very young sheet flows. At a few points, these flows appear to issue from the south flank of the axial ridge, but most appear to have been fed by vents within the depression itself (Ballard et al., 1979). In the eastern portion of the sheet flow plain the lava apparently spilled southward through a gap in the marginal high into the eastern trough along the south wall. A typical cross section of this flow is exhibited by profile 16a (Figure 6). To the east of the spillway the axial ridge is separated from the southern marginal high by older sheet flows derived both from the ridge and from vents in the depression. Small perched sheet flows of the youngest age occur along the north and south flanks of the axial ridge in crestral depressions and valleys.

The northern edge of the axial zone contains small depressions, separated by spurs of pillow lava extending from the ridge. Some, but not all, of the depressions are filled with older sheet flows (Figure 6, profile 4). Only in the extreme northwest region and extending to near the north wall are there extensive sheet flows of a young age.

As Figure 6 and a comparison between Figure 3 and Plate 1 indicate, most sheet flows occupy depressions. Their surfaces, however, are not level. The sheet flows are very extensive, comprising about half of the entire young volcanic zone, in striking contrast to the Famous rift valley, which is almost entirely floored by pillow flows (Ballard and van Andel, 1977b). Within sheet flow areas, structures and flow types are complex (Figure 6) (Ballard et al., 1979).

An extensive area of youngest sheet flows associated with pillow lavas of the same age occurs within the deep graben along the foot of the western south wall. During two dives these flows were observed to have spilled down from the lower north flank of the graben, presumably from fissures associated with the faulting of the marginal high. The young sheet flows in the extreme northwestern corner of this study area may have a similar origin.

The older faulted terrain consists of pillow flows and sheet flows of a configuration similar to the axial ridge but with a topography modified by vertical faulting. Sheet flows occur in depressions, and pillow flows have constructed a complex of volcanoes. The volcanic geology reconstructed by the removal of fault-induced topographic change is indicated in Plate 2. The principal difference of the young axial zone

lies in the absence of extensive sheet flows like those of the southern axial depression. Thus the older terrains are, much like the axial ridge and its northern marginal depression, modified by faulting.

In the Famous rift valley, the central volcanoes are about 200-250 m high and much larger than the individual volcanoes of the Galapagos Rift. Flow directions mapped from the submersible, coupled with an analysis of the detailed topography, enabled Ballard and van Andel (1977b) to determine the growth structure and flow patterns of numerous volcanoes, not only in the axis, but also on the marginal highs and on the terraces beyond. Thus they showed that individual volcanoes are transported laterally in their entirety, retaining their bilateral flow symmetry. The much smaller dimensions and heights of the Galapagos rift volcanoes make that type of analysis more difficult, and our data set includes fewer direct observations of flow directions. Nevertheless, we have attempted to reconstruct the pattern of volcanoes in the same manner, resolving the complex of coalescing edifices of the axial ridge (Plate 2). With much less confidence we made a similar analysis for the volcanoes of the marginal terrain, allowing for structural modifications. The combination of the lobate outlines seen in the topography (Figure 3) within the fault-straightened blocks, and the flow directions seen from Alvin during dives 719, 727, 730, and 735 (Figure 2) show that these older structures have retained the same bilateral flow symmetry of the present axial volcanoes and, except for a reduced height, have the same approximate dimensions.

The entire valley floor is dissected by numerous fissures ranging in width from hairline cracks to small grabens, several meters wide and equally deep. In the axial region, vertical displacement on fissures tends to be negligible (in the tens of centimeters at most), but in the faulted marginal terrain, vertical separations can exceed 20 m. Fissures at the base of fault scarps are common. The fissures occur in bundles or swarms which are only subparallel to the strike of the axis and may deviate up to 30°. There they can be followed over some distance, sometimes several hundred meters, and appear to be quite sinuous. Their sinuosity and continuity are confirmed by Crane's (1978) sidescan sonar data. For some reason, fissuring is mainly restricted to pillow terrain. Of a total of 310 observed fissures, only 10% occur in sheet flows. There also appears to be a relationship between age and degree of fissuring. The densest fissure swarms in the axial region occur in the oldest volcanics in the east and appear to propagate westward. Fissures are virtually absent in the young pillow flows at the western end. Fissure patterns and densities of the marginal zones are not noticeably different from those of the eastern axial ridge, suggesting that the tensional disruption of the new crust is essentially complete when the axial ridge matures.

The hydrothermal springs are located near the present volcanic axis and usually on a pillowed slope near the contact with a young sheet flow (e.g., profiles 10b and 11, Figure 6). Although the pillow flows in spring areas are usually fissured, the springs themselves are not located

on large fissures (Corliss et al., 1979; Ballard and Crane, 1979). We have located five active springs in the crestal area, and Alvin observations suggest two inactive spring sites in older marginal terrain. No springs were found on the western part of the axial ridge.

On four Angus runs we also observed small sediment mounds that resemble, on a reduced scale, the sediment mound hydrothermal field of the south flank of the Galapagos Rift between 0°35'N and 0°39'N (Lonsdale, 1977; Corliss et al., 1979). These minimounds occur in both marginal zones (Plate 1), in rather heavily sedimented terrain. The apparently hydrothermal deposits exhibit a variety of colors including brown, yellow, and orange. The minimounds are conical in shape and stand approximately 1-2 m high. If they are, indeed, the equivalent of the hydrothermal mound field on the south flank of the Galapagos Rift, they demonstrate continued hydrothermal activity beyond the zone of present volcanic activity. In addition to these minimounds the rift valley study area contains numerous smaller-scale deposits of a similar color range. The youngest southern sheet flows between the axial pillowed ridge and southern marginal high contain many small deposits of bright yellow material within the folds of the sheet flows. The young sheet flows within the southern depression at the base of the south wall commonly have yellow, brown, and orange stains around the base of the lobate sheet forms. In general, the apparent hydrothermal activity within the rift valley can be grouped into four basic categories: (1) warm water vents located along the central volcanic ridge, (2) staining around the base of fresh glassy lava forms, (3) bright yellow deposits in small pockets within the young sheet flows, and (4) minimounds within the zone of heavy sedimentation in the southern and northern marginal highs.

A small seamount is located just north of the center of the south wall. As far as we can ascertain, it is of the same age as the rest of the marginal terrain, but it has a very distinct lava type distinguished by a peculiar alteration best described by the word 'moldy'.

The glass covering the pillow flows that make up this seamount exhibits this unusual form of alteration. The glass on the steep sides of an individual pillow has fallen off and accumulated at its base. This black material mixed with the white-to-brown pelagic sediments is responsible for the moldy appearance. The glass on the top surfaces of the pillows is still present, although it appears to have separated from the pillow itself. The pillows therefore have black tops and white sides where the white, altered interior is exposed, also adding to the moldy appearance. All runs traversing flows from this seamount show this distinctive alteration, and sediments to some distance from the seamount contain significant amounts of the highly characteristic detritus (Plate 2).

Geological Observations Pertinent to Explanatory Models

Sleep and Rosendahl (1979) have drawn attention to the uses and limitations of kinematic models based on surface observations. Below,

we shall present a diagrammatic geologic model in an attempt to account for the observations discussed above. In doing so we are aware of the limitations of a purely geologic model; we do not feel in a position to integrate this model with the various dynamic models proposed for the midocean rift valley, such as those of Sleep and Rosendahl (1979) and have not been able to extend our discussion to such relevant phenomena as stress trajectories. It is our hope that the following discussion may inspire others to the development of dynamic models that take into account the results of our study. Before we proceed to a geologic interpretation, we list below what appear to us to be the relevant observations and constraints.

Most of the key observations refer to the striking geological, morphological, and structural asymmetry in the presence of a near-perfect spreading rate symmetry:

1. The volcanic axis is located about 0.5 km north of the topographic and structural axis of the rift valley, which coincides with the center of the young zone of sheet flows south of the volcanic ridge.

2. The northern marginal high is close to the volcanic ridge and north wall and higher than the volcanic ridge. The southern marginal high, on the other hand, is wider than, but at about the same elevation as, the volcanic axial ridge and separated from the south wall by broad and deep depressions.

3. A broad, low-lying zone of youngest sheet flows separates the axial volcanic ridge from the southern marginal high. Between the axial volcanic ridge and the northern marginal high, a narrow zone occurs which contains young pillow flows forming topographic spurs. The depressions between these spurs are commonly filled with sheet flows older than the pillow flows making up the spurs and much older than the southern sheet flows. On a more regional basis the asymmetry is also prominent, both across and along the strike of the Galapagos Ridge.

4. Along the entire surveyed length of the crest (85°25' to 86°17'W) as well as on the lineaments of the ridge flanks, a low in one marginal high or lineament opposes a high in the corresponding marginal high or lineament on the other side of the rift axis.

5. Flank lineaments are paired across the rift axis and are similar in detail on opposite sides. This is true except for the youngest sheet flow area on the south side, which corresponds to a rather ill formed lineament represented by the axial volcanic ridge and northern marginal high in the rift valley.

6. Several unpaired elements occur within the rift valleys. There is only one young volcanic high and only one major sheet flow depression.

The following observations concerning the nature of the volcanic terrain are important:

1. If we disregard the extensive sheet flows south of the axial ridge, the areal ratio of pillow flows to sheet flows is about the same in the axial ridge and the marginal highs, even if we assume that all terrain which is totally sediment covered consists of sheet flows (Plate 2). This is also true for the narrow trough-and-spur zone between the axial ridge and the northern marginal zone.

2. Pillow flows form the constructional highs. Sheet flows occur in valleys and depressions and only rarely on volcano flanks. The larger sheet flows are younger than most pillow flows and were fed from vents within the sheet flow areas, not from the pillowed volcanoes.

3. Reconstruction of flow forms and flow directions suggests that the marginal zones consist of individual volcanoes similar in dimensions (although perhaps reduced in height) to those of the axial ridge. The intact volcanic units imply that after a constructional period ends, extension, rifting, and crustal accretion resume to one side or the other of the completed volcanic ridge.

Structurally, the following conclusions need to be considered:

1. Tensional fissures are common only in pillow flows. Even in the oldest sheet flows they are rare. Fissures are sinuous and often long and occur in swarms. Individual fissures and swarms are subparallel to the axial strike, deviating from it as much as 30°.

2. The youngest, western end of the axial ridge is not fissured, but at the older, eastern end, fissuring density is not measurably different from that of the marginal zones, suggesting that tensional disruption is completed early and that the fissuring is propagating westward.

3. Faulting begins abruptly at the edges of the young volcanic zone and marks a major age discontinuity. Faults occur in bundles, and single scarps are often composed of step faults. Faults are subparallel to the regional strike, and their en echelon arrangement produces alternating horsts and grabens in the marginal zones along strike.

4. Less uplift occurs on faults in the northern marginal zone than in its southern counterpart.

Several important age relationships can be inferred:

1. The axial ridge is older and better developed in the east than in the west. The resulting topographic variation, alternately high and low along strike, can be observed along the entire surveyed portion of the rift axis.

2. The sheet flows in the trough south of the axial ridge are among the youngest flows in the rift valley and are decidedly younger than most pillow flows of the axial ridge.

3. Young volcanism is not restricted to the axial zones. Extensive young sheet flows, probably coming from the flanks of the marginal highs, occur along the south wall and near the northeastern portion of the north wall. In terms of area and volume, however, they are not comparable to those of the axial zone.

4. There is a large age discontinuity between the axial zone and the adjacent rocks of the marginal highs, especially in the south.

5. The best estimate for the age of the youngest flows in the valley is less than 100 years. The total age range of the exposed volcanics in the axial zone may be a few thousand years, compared to an inferred crustal age of 100,000 years at the walls.

Finally, we note that hydrothermal springs are widespread and usually occur on pillow slopes above a low containing younger sheet flows. The

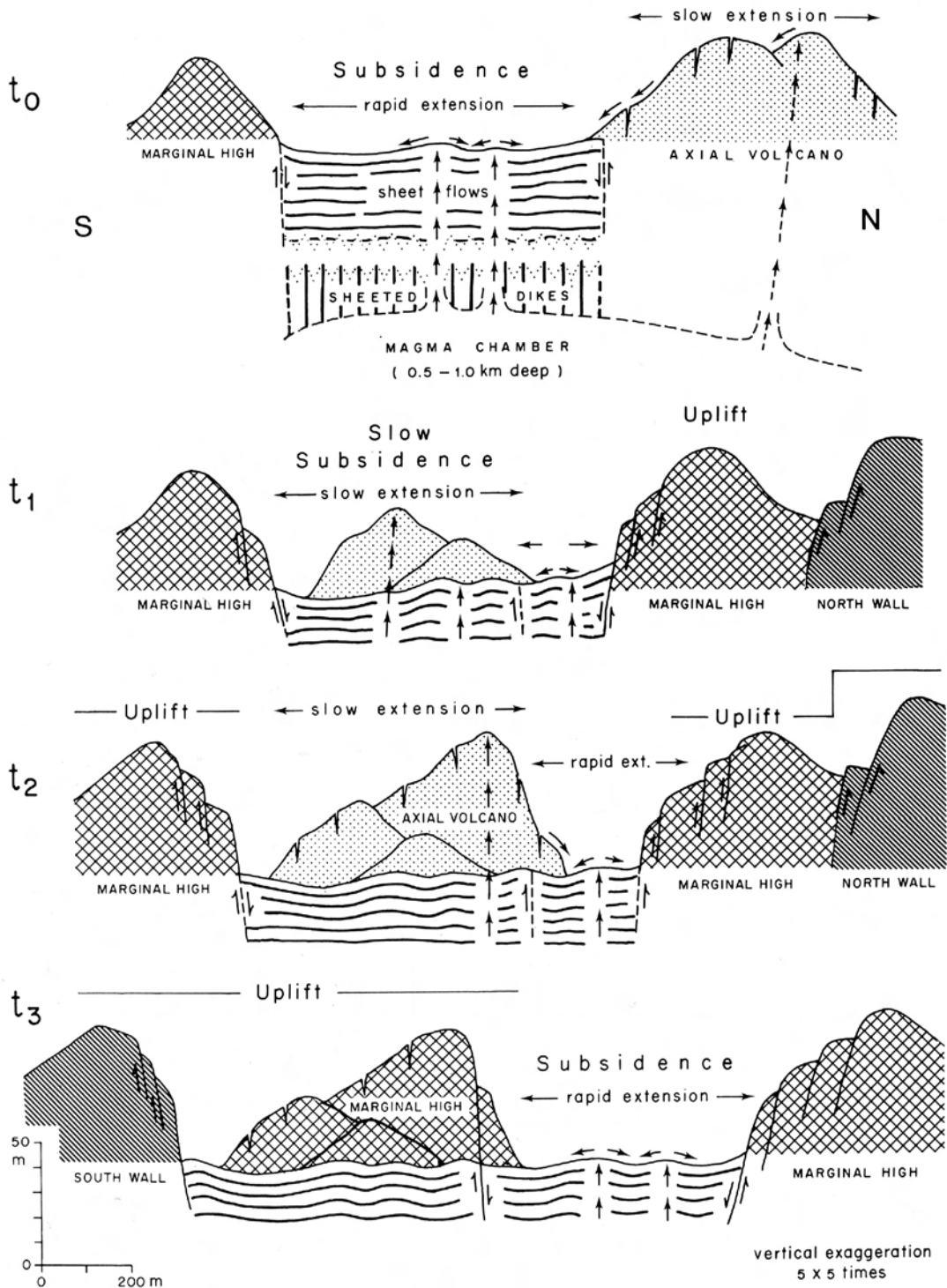


Fig. 7. Sketches illustrating proposed volcanic and structural evolution of the Galapagos rift valley. Terrain outlines derived directly from topographic cross sections: dotted, pillow basalts; horizontal lines, sheet flows; drawn vertical arrows, rapid lava transport; dashed arrows, slow lava transport. For discussion, see text.

vents occur in fissured areas and are found only in the older part of the active axial volcanic ridge. Two much older, inactive spring sites occur in the marginal zones. Four minimounds, as yet of questionable significance, may indicate the existence of hydrothermal activity outside the present volcanic axis.

Evolution of the Rift Valley

We shall now attempt to reconstruct the volcanic and structural evolution of the Galapagos Rift valley, taking into account as many of the observations and constraints listed above as possible. The kinematic model we propose is

a further elaboration of the model we suggested for the inner rift valley in the Famous area (Ballard and van Andel, 1977b) except that it involves a faster spreading ridge. We see nothing in our new evidence that invalidates the principles of that model but recognize that it is only one of several possible models permitted by the data.

Most models proposed for the evolution of the midocean ridge crest attempt either to match the observed topography with models based on theory and on extrapolated physical properties of the crust or to reconstruct the crustal evolution with the aid of vertical rock sections derived from obducted ophiolites. We cite Sleep and Rosendahl (1979) as perhaps the most successful example of the first and Cann (1974) and Kidd (1977) as typical of the second. Both kinds of models typically assume continuity in time and space for both the sequence of events and the formation of newly formed crust, although the existence of discontinuities across faults is generally recognized. Our model is distinct in that we specifically postulate a discontinuous eruptive and deformational history and generate the crust (perhaps with the exception of the magma chamber and the zone just above) in discrete blocks defined by eruptive units (volcanoes) and later by boundary faults.

We emphasize that our model deals only with the evolution within the rift valley. Although we favor models for the origin of the rift valley-crestal range complex that bring into play the viscous head loss arguments of Sleep and others, our observations shed no additional light on this problem.

The proposed kinematic history, presented in Figure 7, is based on suitably chosen topographic cross sections of the rift valley which we combine to create the valley profile at some future time after one additional volcanic cycle has taken place.

The postulated sequence (Figure 7, t_0) begins with rapid extension and extensive intrusion of sheeted dikes in a wide depression above a shallow magma chamber. Sheet flows issue copiously from vent zones subparallel to the strike (Ballard et al., 1979), concealing evidence of earlier extension. The zone subsides rapidly along boundary faults and fills with an appreciable thickness (several hundred meters) of sheet flows. On the right the depression is bordered by an axial volcanic ridge of decreasing pillow flow activity. The boundary fault is therefore masked by pillow flow aprons. On the south lies a marginal high which maintains its position as the depression subsides.

At time t_1 , rapid extension in this part of the rift valley has ceased as the roof of the magma chamber has thickened greatly (perhaps doubled in thickness), owing in part to the accumulation of sheet flows. Volcanic activity has reduced to a slow buildup of pillowed volcanoes in several stages. Modest subsidence occurs, and some extension continues which gives rise to extensive fissuring, hydrothermal circulation, and the formation of warm springs. A new zone of rapid extension begins to form to the right (or left) of the axial volcanic ridge in the thinner zone between the base of the volcanic ridge and the northern marginal high.

Thus the spreading rate can, but need not, remain constant. The northern and southern marginal highs undergo isostatic uplift as a consequence of the thickening process occurring in the roof of the magma chamber.

At time t_2 the buildup of the axial ridge is nearly complete. The northern sheet flow depression has widened, and its southern boundary fault is now masked with pillow flows from the volcanic ridge. Finally (t_3), the former axial ridge has become extinct and is part of the southern marginal high, rising rapidly in response to isostatic uplift. The former southern marginal high itself is now the south wall. Rapid extension occurs in the sheet flow depression north of the former axis. The northern marginal high, close to the zone of hot, upwelling magma, is stable. The sheet flow depression is subsiding rapidly. In all, the inner valley comprises about six to eight volcanic zones. Given the magnetic age at the walls, a complete cycle must therefore last on the order of 10,000 years. The flow complex presently exposed in the valley indicates that a new volcanic cycle has just begun with the initial outpouring of fresh and extensive sheet flows. During this time we have rapid extension, the formation of sheet flows, and subsidence above a shallow magma chamber (perhaps 0.5 km (Rosendahl, 1976)). Subsidence takes place on normal faults. The cycle ends with a period of pillow flows forming an axial volcanic ridge on which extensive fissuring produces the opportunity for hydrothermal circulation. The cycle comes to an end when the crust has become too thick, and it is easier for rifting to shift to a new zone of rapid extension. Sheet flows then form to one side or the other of the previous site in a linear area of structural weakness. The old volcanic axis is uplifted by isostatic compensation over the deeper and cooler part of the magma chamber and eventually becomes part of the flanking wall.

This model is in accord with the observations summarized in the previous section but does not explain or require all of them. We have not explained the occurrence of recent volcanism in the marginal regions but think this is associated with displacement along the major boundary faults. We have found that recent volcanism in those areas occurs only as sheet flows at the base of major fault scarps. The model is also an oversimplification. The variation in age and volcanic character along the strike of the axial volcanic ridge shows that at any one time, various segments of the rift valley are in slightly different stages of activity. We assume that this may be due to the apparent shoaling and deepening of the magma chamber along the axis postulated by Crane (1978) and Allmendinger and Riis (1979). Our data cover too short a segment of the rift axis to know if we are seeing different stages of the same cycle or different cycles themselves.

The model also does not touch on the intriguing opposition across the rift axis of highs and lows in the marginal highs, the crest ranges, and the lineaments of the ridge flanks. The best explanation, suggested by Crane (1978), is that the magma chambers may be located slightly off axis and that eruptions on the surface from

any of them will tend to lower the opposite side. Our data, however, do not provide further insight or evidence to support Crane's idea or the complex system of downwarps and upwarps that she infers from it.

In fact, we have assumed no warping or bending of the new crust at all, in contrast with models such as those of Cann (1974) and Kidd (1977), which show crustal layers dipping toward and faults dipping away from the axis. The evidence for such downwarping, which rests mainly on magnetic data in drill holes, is slim and rather ambiguous. For the time being therefore we prefer the simple model of uplift and subsidence along normal faults with flat-lying or very shallow dipping crustal layers.

Our model postulates a thick section of sheet flows beneath the surface pillowed flows. Sheet flows, commonly in layers from a few centimeters to a few meters, have been frequently encountered in Pacific crustal drilling (Hekinian et al., 1977; Yeats and Hart, 1974). In the walls of the Galapagos Rift, where fault planes generally expose less than 50-100 m of section, we do not usually observe a major sheet flow sequence, but with a total thickness of the central pillow buildup of that amount, such is not to be expected. Only in one site, on dive 731, at the foot of the large southern boundary scarp of the southern marginal high, were massive, horizontally layered basalt units seen. On the other hand, in the Famous area, where exclusively pillow basalts were observed on the surface, several hundred meters of massive horizontal basalt sheets were seen in the western boundary fault below 300 m of pillow basalts. This thickness is equivalent to the height of the axial volcanoes (Ballard and van Andel, 1977b). It seems possible therefore that in the Famous area as well, the extrusive sequence begins with a series of sheet flows, but the result of its slower spreading rate is that the pillow flows have more time to cover the earlier sheet flows before the newly formed crust is transported beyond the central zone of volcanic activity.

Acknowledgments. This study has been supported, through subcontracts from Oregon State University to Stanford University and the Woods Hole Oceanographic Institution, by grant OCE75-23352 of the Office of the International Decade of Ocean Exploration at the National Science Foundation. We thank our colleagues in the Galapagos Hydrothermal Project, the Alvin and Angus teams, and the officers and crews of the R/V Lulu and Knorr for their generous assistance in the acquisition of the data. We have been greatly assisted in the data processing by Christine Wooding and Catherine Scheer. Kathleen Crane's experience in the area from the 1976 expedition has been most helpful, as well as her assistance in our 1977 field program. We have further benefited greatly from comments and discussion by Burce R. Rosendahl and Robin T. Holcomb. The art work contained in this paper was done by Dorothy Meinert of Woods Hole. We would also like to thank the Naval Oceanographic Office for the support they gave us by surveying the area with one of their advanced multibeam sonar systems. Woods Hole Oceanographic Institution contribution 4204.

References

- Allmendinger, R. V., and F. Riis, The Galapagos Rift at 86°W, 1, Regional morphological and structural analysis, *J. Geophys. Res.*, **84**, in press, 1979.
- Ballard, R. D., and J. G. Moore, *Photographic Atlas of the Mid-Atlantic Ridge*, 114 pp., Springer, New York, 1977.
- Ballard, R. D., and Tj. H. van Andel, Project Famous: Operational techniques and American submersible operations, *Geol. Soc. Amer. Bull.*, **88**, 495-506, 1977a.
- Ballard, R. D., and Tj. H. van Andel, Morphology and tectonics of the inner rift valley at lat. 36°50'N on the Mid-Atlantic Ridge, *Geol. Soc. Amer. Bull.*, **88**, 507-530, 1977b.
- Ballard, R. D., R. T. Holcomb, and Tj. H. van Andel, The Galapagos Rift at 86°W, 3, Sheet flows, collapse pits, and lava lakes of the rift valley, *J. Geophys. Res.*, **84**, in press, 1979.
- Bryan, W. B., and J. G. Moore, Compositional variations of young basalts in the Mid-Atlantic rift valley near 36°49'N, *Geol. Soc. Amer. Bull.*, **88**, 556-570, 1977.
- Cann, J. R., A model for oceanic crustal structure developed, *Geophys. J. Roy. Astron. Soc.*, **39**, 169-188, 1974.
- Corliss, J. D., R. D. Ballard, K. Crane, J. Dymond, J. D. Edmond, Tj. H. van Andel, R. P. Von Herzen, and D. L. Williams, Hydrothermal warm springs on the Galapagos Rift, *Science*, 1979.
- Crane, K., Structure and tectonogenesis of the Galapagos inner rift, 86°10'W, *J. Geol.*, **86**, 715-730, 1978.
- Crane, K., The Galapagos Rift at 86°W, 5, Morphological wave forms, submitted to *J. Geophys. Res.*, 1979.
- Crane, K., and R. D. Ballard, The Galapagos Rift at 86°W, 4, Structure and morphology of hydrothermal fields, submitted to *J. Geophys. Res.*, 1979.
- Detrick, R. S., D. L. Williams, J. D. Mudie, and J. G. Sclater, The Galapagos spreading center: Bottom water temperature variation, and the significance of geothermal heating, *Geophys. J. Roy. Astron. Soc.*, **38**, 627-638, 1974.
- Glenn, M. F., Introducing an operational multi-beam-array sonar, *Int. Hydrogr. Rev.*, **47**, 35-40, 1970.
- Hekinian, R., and M. Hoffert, Rate of palagonitization and manganese coating on basaltic rocks from the rift valley in the Atlantic Ocean near 36°50'N, *Mar. Geol.*, **19**, 91-100, 1975.
- Hekinian, R., et al., *Glomar Challenger* completes 54th cruise, *Geotimes*, **22**, 19-25, 1977.
- Hey, R., Tectonic evolution of the Cocos-Nazca spreading center, *Geol. Soc. Amer. Bull.*, **88**, 1404-1420, 1977.
- Hey, R., G. L. Johnson, and A. Lowrie, Recent plate movements in the Galapagos area, *Geol. Soc. Amer. Bull.*, **88**, 1385-1403, 1977.
- Kidd, R. G. W., A model for the process of formation of the upper oceanic crust, *Geophys. J. Roy. Astron. Soc.*, **50**, 149-183, 1977.
- Klitgord, K. D., and J. D. Mudie, The Galapagos spreading center: A near-bottom geophysical survey, *Geophys. J. Roy. Astron. Soc.*, **38**, 563-587, 1974.

- Lonsdale, P. F., Abyssal pahoehoe with lava whorls at the Galapagos Rift, Geology, 5, 147-152, 1974.
- Lonsdale, P. F., Deep-tow observations at the mounds abyssal hydrothermal field, Galapagos Rift, Earth Planet. Sci. Lett., 36, 92-110, 1977.
- Macdonald, K. C., B. P. Luyendyk, J. D. Mudie, and F. N. Spiess, Near-bottom geophysical study of the Mid-Atlantic Ridge median valley near lat. 37°N, Geology, 3, 211-215, 1975.
- Moore, T. C., Jr., G. R. Heath, and R. O. Kowsmann, Biogenic sediments of the Panama Basin, J. Geol., 81, 458-472, 1973.
- Needham, H. D., and J. Francheteau, Some characteristics of the rift valley in the Atlantic Ocean near 36°48'N, Earth Planet. Sci. Lett., 22, 29-43, 1974.
- Phillips, J. D., and H. S. Fleming, Multibeam sonar study of the Mid-Atlantic Ridge rift valley, 36°-37°N, Map Ser. MC-19, Geol. Soc. of Amer., Boulder, Colo., 1978.
- Ramberg, I. D., and Tj. H. van Andel, Morphology and tectonic evolution of the rift valley at lat. 36°30'N, Mid-Atlantic Ridge, Geol. Soc. Amer. Bull., 88, 577-586, 1977.
- Rosendahl, B. R., Evolution of the oceanic crust, 2, Constraints, implications, and inferences, J. Geophys. Res., 81, 5305-5314, 1976.
- Sclater, J. G., and J. Francheteau, The implications of terrestrial heat flow observations on current tectonic and geochemical models of the crust and upper mantle of the earth, Geophys. J. Roy. Astron. Soc., 20, 509-542, 1970.
- Sclater, J. G., and K. D. Klitgord, A detailed heat flow, topographic and magnetic survey across the Galapagos spreading center at 86°W, J. Geophys. Res., 78, 6951-6976, 1973.
- Sclater, J. G., R. P. Von Herzen, D. L. Williams, R. N. Anderson, and K. D. Klitgord, The Galapagos spreading center, heat flow low on the north flanks, Geophys. J. Roy. Astron. Soc., 38, 609-626, 1974.
- Sleep, N. H., and B. R. Rosendahl, Topography and tectonics of mid-ocean ridge axes, J. Geophys. Res., 84, in press, 1979.
- Storzer, M. D., and M. Selo, Ages par la méthode de traces du fission de basaltes prélevés dans la vallée axiale de la dorsale médio-atlantique aux environs de 37°N, C. R. Acad. Sci., 279-D 1649-1651, 1974.
- Swift, S. A., Holocene rates of sediment accumulation in the Panama Basin, eastern equatorial Pacific: Pelagic sedimentation and lateral transport, J. Geol., 85, 301-320, 1977.
- van Andel, Tj. H., Texture and dispersal of sediments in the Panama Basin, J. Geol., 81, 434-457, 1973.
- van Andel, Tj. H., G. R. Heath, B. T. Malfait, D. F. Heinrichs, and J. I. Ewing, Tectonics of the Panama Basin, eastern equatorial Pacific, Geol. Soc. Amer. Bull., 82, 1489-1508, 1971.
- van Andel, Tj. H., G. R. Heath, and T. C. Moore, Jr., Cenozoic history and paleo-oceanography of the central equatorial Pacific Ocean, Geol. Soc. Amer. Mem., 143, 135 pp., 1975.
- Weiss, R. F., P. Lonsdale, J. E. Lupton, A. E. Bainbridge, and H. Craig, Hydrothermal plumes in the Galapagos Rift, Nature, 267, 600, 1977.
- Williams, D. L., R. P. Von Herzen, J. G. Sclater, and R. N. Anderson, The Galapagos spreading center: Lithospheric cooling and hydrothermal circulation, Geophys. J. Roy. Astron. Soc., 38, 587-608, 1974.
- Yeats, R. S., W. C. Forbes, K. F. Scheidegger, G. R. Heath, and Tj. H. van Andel, Core from Cretaceous basalt, central equatorial Pacific, Leg 16, Deep Sea Drilling Project, Geol. Soc. Amer. Bull., 84, 871-882, 1973.
- Yeats, R. S., and S. R. Hart, Initial Reports of the Deep Sea Drilling Project, vol. 34, 814 pp., U.S. Government Printing Office, Washington, D. C., 1974.

(Received July 26, 1978;
revised January 8, 1979;
accepted January 30, 1979.)